ARSENAZO III-Ca^{2+}

Effect of pH, Ionic Strength, and Arsenazo III Concentration on Equilibrium Binding Evaluated with Ca^{2+} Ion-sensitive Electrodes and Absorbance Measurements

H. Mack Brown and Bo Rydqvist, *Department of Physiology, University of Utah College of Medicine, Salt Lake City, Utah 84108*

ABSTRACT Equilibrium binding properties of the metallochromic indicator Arsenazo III (AIII) were characterized by Ca^{2+} and acid/base titration. Free calcium was measured directly with Ca^{2+} ion-sensitive electrodes. Absorbance changes were measured by both a conventional scanning spectrophotometer and a dual wavelength spectrophotometer. Acid/base titration of AIII in conjunction with Ca^{2+} ion-sensitive electrode measurement and absorbance changes indicate that pH can change AIII absorbance through a change of the K_D for Ca-AIII formation, and, in addition, that there is a pH-specific component that is not dependent on Ca-AIII formation. The dissociation constant (K_D) of AIII varied not only with pH, but with ionic strength and AIII concentration. Studies conducted to examine AIII-Ca stoichiometry resulted in different initial conclusions, depending on the method of analysis. Log ΔA-log AIII relations were in accord with previously published results, which indicates that more than one AIII binds to one Ca^{2+} ion. But Job plots, Scatchard analysis, and Hill plots all indicated 1:1 binding. The method of absorbance measurement, i.e., scanning or dual wavelength did not influence the results. These findings were reconciled on the basis of changes in K_D with AIII concentration and ionic strength. In 200 mM KCl, K_D of AIII-Ca varies by a factor of 7 between $10^{-4.3}$ and 10^{-3} M AIII. Thus, a disproportionately large amount of Ca-AIII is formed as AIII concentration is increased, which results in slopes greater than unity for log ΔA-log AIII relations.

INTRODUCTION

Arsenazo III (AIII) has been widely used as an indicator for free-Ca^{2+} changes in single-cell preparations (Brinley et al., 1977; Brown et al., 1977; Gorman and Thomas, 1978; Scarpa, 1979; Ahmed and Connor, 1980). Despite the apparent sensitivity and speed of the method for the detection of small changes in free Ca^{2+}, there are difficulties in interpreting the absorbance changes quantitatively. The two most significant problems that have evolved in application of the dye to physiological problems are (*a*) dependency of absorbance changes on pH changes (Buděšinský, 1969*a*; Ogan and Simons, 1979), and (*b*) the question of whether or not the dye forms 1:1 or 2:1 complexes with Ca^{2+} under physiological conditions (Michaylova and Ilkova, 1971; Gratzer and Beaven, 1977; Gorman and Thomas, 1978; Thomas, 1979; Ahmed et al., 1980). A change in pH may occur concomitantly with intracellular Ca^{2+} changes in a number of physiological processes. For this reason, the nature of absorbance

changes that are dependent on pH needs to be clearly established. It has been demonstrated that a micromolar change in protons can produce an absorbance change at the most sensitive Ca^{2+} wavelength (654 nm), which is 30 times greater than an equivalent change in the Ca^{2+} concentration. An additional complication is that a change in the buffer system at constant pH and Ca^{2+} can produce changes that mimic Ca^{2+} changes (Ogan and Simons, 1979).

The problem of complex formation is crucial for the quantitative determination of free-Ca^{2+} changes based on observed absorbance changes of a cell injected with AIII. This is best illustrated by a simple example. For a given observed change of absorbance ($\Delta A = 0.01$) in a cell injected with 0.75 mM dye, a change of Ca_f on the order of 3.5×10^{-6} would be calculated with dissociation constants for 1:1 binding of AIII that are commonly reported in the literature ($K_D \sim 30$ μM; Brinley et al., 1977; Ogan and Simons, 1979; Owen and Brown, 1979). On the other hand, if 2:1 binding occurs, the same ΔA would yield a calculated Ca_f of 2.8×10^{-7} M, if the K_{D_2} ($K_1 \cdot K_2 = 1.8 \times 10^{-9}$ M^2) reported by Thomas (1979) is used for the calculation.

The major evidence for 2:1 complexing rests on the relation between log absorbance changes and log AIII concentration at a fixed free Ca^{2+} concentration. Gorman and Thomas (1978) and Thomas (1979) obtained a slope of 2 from such a relation, demonstrating that two AIII molecules complex one Ca^{2+} ion. Ahmed et al. (1980), unable to confirm this result, obtained a slope of 1 from a similar experiment. They were unable to reconcile this discrepancy but did raise the possibility that differences in absorbance measurement techniques may have accounted for the discrepancy, i.e., dual-wavelength spectrophotometer vs. a more conventional scanning spectrophotometer. These same authors provided additional evidence for 1:1 binding, the most compelling of which was a Job plot.

From the above, there remain several unresolved problems concerning AIII-Ca stoichiometry: (*a*) The type of spectrophotometer may be critical; this is a possibility since filter photometers integrate over a broader wavelength band than most scanning units. (*b*) Free Ca^{2+} is usually not measured directly in investigations of AIII, this may have contributed to some disparity in results. (*c*) pH may exert a direct effect on absorbance by changing Ca-AIII formation, or non-Ca^{2+} factors may be involved in pH absorbance changes.

The approach used in investigating these problems was titration of an AIII solution with acid, base, or $CaCl_2$, while measuring changes in free Ca^{2+} with a Ca^{2+}-ISE (ion-sensitive electrode) (Brown et al., 1976). During titration the absorption spectrum of the solution was determined in a Cary model 11 recording spectrophotometer and in addition the absorbance difference at selected wavelength pairs was measured with a differential wavelength spectrophotometer (Chance, 1972; Gorman and Thomas, 1978; Scarpa, 1979). The latter measurements were conducted under conditions similar to those experienced in recording absorbance changes from single cells. We are able to confirm the results of Gorman and Thomas (1978) and Thomas (1979) but we disagree with their conclusion that this result represents 2:1 binding stoichiometry. Rather, the present results indicate that the K_D of AIII varies as a function of AIII concentration and ionic strength, and that the log ΔA-log AIII relation has a slope greater than unity for these reasons. Other analyses both from absorbance measurements and Ca^{2+} electrode measurements indicates that the correct binding stoichiometry is 1:1.

MATERIALS AND METHODS

Chemicals

AIII was purified from crude AIII (Sigma Chemical Co., St. Louis, Mo., lot 105-01011) with a modified acid precipitation method (Savvin, 1964; Buděšinský, 1969*b*; Gratzer and Beaven, 1977). The following step was added to the procedure described by these authors. The dye was dissolved in hot NaOH (1 N), and after cooling and titration to pH 7.5 with concentrated HCl, the solution was passed through a Chelex-100 column (25 cm; Biorad Labs, Richmond, Calif.), which yields a highly purified AIII. The extinction coefficient at 650 nm ($\Delta\epsilon_{650}$) of a 50-μM solution of a typical batch at pH 7.25 was $2.64 \times 10^4\ M^{-1}\ cm^{-1}$ (see Fig. 1 and Eq. 6). $\Delta\epsilon_{650}$ varied slightly between batches. A small Ca^{2+} impurity (0.6%) was estimated from the spectrophotometric data. Purified AIII from Sigma Chemical Co. (lot 99C-7060) yielded $\Delta\epsilon_{650} = 2.04 \times 10^4\ M^{-1}\ cm^{-1}$ for the same conditions. The potassium chloride (KCl) used in the present experiments had a Ca^{2+} impurity of 0.005% (including other divalent ions). In a solution of 200 mM KCl, this will give a maximal total Ca^{2+} concentration of $\sim 5 \times 10^{-6}$ M. The contribution of divalent ions by Hepes, EGTA, and other buffers was neglected. Deionized water (Milli Q, Millipore Corp., Bedford, Mass.) was used to prepare all solutions. Atomic absorption analysis of this water yielded total $Ca^{2+} < 10^{-9}$ M (Owen and Brown, 1979).

pH and Ca^{2+} Titrations

AIII solutions were titrated by adding, HCl, KOH, or $CaCl_2$. The AIII solutions, usually 200 ml, were mixed by continuous stirring with a magnetic stirrer. The pH was monitored with a Corning pH electrode (Corning Glass Works, Science Products Div., model 476051) connected to a Varactor bridge amplifier (Analog Devices; Norwood, Mass.) ($Z_i = 10^{14}\ \Omega$). The Ca^{2+} concentration was monitored with

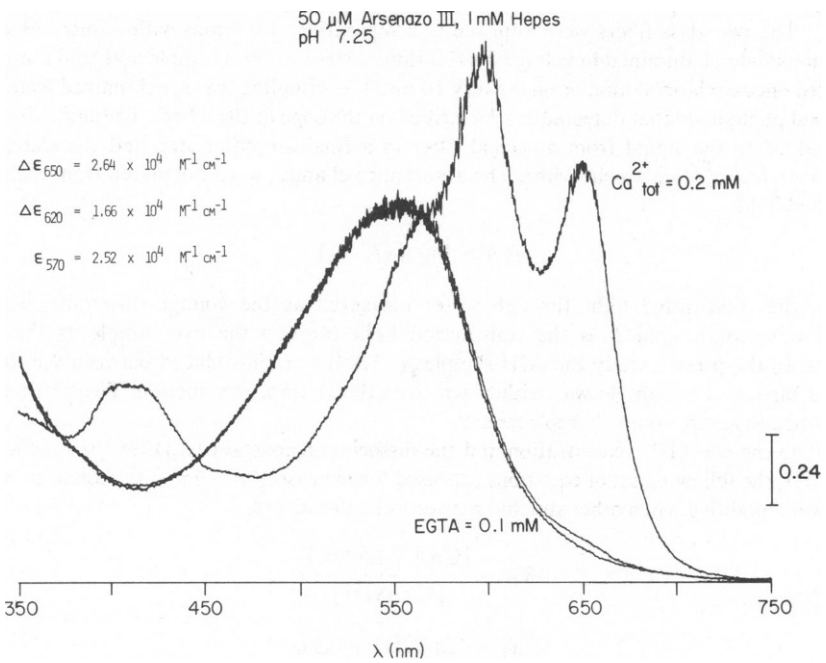

FIGURE 1 Absorption spectra of purified AIII in solution (middle trace at 650 nm), AIII plus EGTA (bottom trace), and AIII with an excess Ca (top trace). Extinction coefficients (ϵ_λ) are shown in the in the inset.

a 1-mm Ca-ISE (Brown, Pemberton and Owen, 1976; provided by Nuestro Research, Inc. Salt Lake City, Utah) connected to a second Varactor bridge amplifier. Reference electrode consisted of a saturated KCl-Ag/AgCl half-cell in contact with the solution via a fritted glass plug. A digital voltmeter and a pen writer was used to record the two signals. The pH electrode was calibrated according to commercially available pH standards. Calibration of the Ca-ISE in the high ionic strength solutions (containing 50 mM KCl or 200 mM KCl) has been described previously (Brown et al., 1976). The presence of AIII in these solutions did not affect the performance of the electrode. Solutions of AIII at low ionic strength, i.e., pure AIII to which small amounts of Ca^{2+} were added, required special consideration. These solutions produced a systematic positive offset from calibration curves that were routinely obtained with background K^+. To calibrate the electrode in a given AIII solution, an excess of $CaCl_2$ was added to the solution, so that a known free Ca^{2+} could be determined. This established a V_{Ca}-pCa point for the electrode and the experimentally determined $\Delta V_{Ca}/\Delta$pCa relation in 10 mM KCl was then used to determine pCa values in the test solutions.

Absorbance Measurements

A Cary model 11 spectrophotometer (Cary Instruments, Fairfield, N.J.) was used to obtain continuous absorption spectra. Cuvettes with a pathlength of 1, 5, and 10 mm were used, depending on the concentration of the dye. Measurements were also performed with a dual-wavelength microspectrophotometer (μ-spec) (cf. Gorman and Thomas, 1978), which has been used for absorbance measurements in isolated cells (Brown and Rydqvist, 1980 *a*, *b*; Rydqvist and Brown, 1980). The light from a 100-W Halogen lamp was projected onto a rotating wheel containing six interference filters (Ditric Optics, Hudson, Mass; 1/2 intensity bandwidth 10 nm); the wheel was rotated at ~-6,000 rpm. Light was led from the wheel via a fiber optic bundle and focused with a microscope objective onto an 80-μm glass fiber in the experimental chamber. A second fiber of the same size was used to gather the incident light and to project it onto a photodiode (United Detector Technology Inc., Santa Monica, Calif., model PIN-020A). The two glass fibers were adjusted to a separation of 0.1 mm with a micrometer. Signals from the photodiode, maintained in voltage configuration, were fed into sample and hold amplifiers that were updated once each revolution or once every 10 ms. The sampling was synchronized from the signal from a second photodiode that detected marks scribed on the edge of the wheel. The signal from any one filter was added to the signal from a second filter in a final amplifier step and the changes in this difference were recorded on a pen writer. The absorbance changes were calculated from measurements of transmitted light:

$$\Delta A = \log_{10}(I_1/I_2), \tag{1}$$

where I_1 is the transmitted light through water measured as the voltage difference between two preselected wavelengths and I_2 is the transmitted light through the dye sample at the same two wavelengths. In the present study the AIII samples (~1 ml) were introduced between the fibers of the μ-spec via a pipette. The sample was withdrawn from the chamber by suction. Two or three changes were performed to assure complete replacement.

To calculate the Ca-AIII concentration and the dissociation constant (K_D) for the reaction between Ca^{2+} and AIII, the following set of equations was used for the case of n = one Ca^{2+} bound to AIII. These equations were modified when other stoichiometries were considered.

$$K_D = \frac{[Ca_f] \cdot [AIII_f]}{[Ca\text{-}AIII]}, \tag{2}$$

$$Ca_T = Ca\text{-}AIII + Ca_f, \tag{3}$$

$$AIII_T = Ca\text{-}AIII + AIII_f, \tag{4}$$

$$\frac{\Delta A}{\ell \cdot \Delta\epsilon_\lambda} = [Ca\text{-}AIII], \tag{5}$$

where ℓ is the pathlength

$$\Delta\epsilon_\lambda = \epsilon_\lambda\,(\text{Ca-AIII}) - \epsilon_\lambda\,(\text{AIII})\ (\text{M}^{-1}\,\text{cm}^{-1}), \tag{6}$$

where ϵ_λ (Ca-AIII) is the molar extinction coefficient for the Ca-dye complex and ϵ_λ AIII is the molar extinction coefficient for the dye alone at the wavelength λ and

$$\text{Ca}_\text{T} = \text{Ca}^{2+}_\text{total}, \qquad \text{AIII}_\text{f} = \text{AIII}_\text{free},$$
$$\text{Ca}_\text{f} = \text{Ca}^{2+}_\text{free}, \qquad \text{AIII}_\text{T} = \text{AIII}_\text{total}.$$

RESULTS

Job Plots

Fig. 2*A* shows Job plots (Job, 1928) obtained from measurements with Ca-ISE and from absorbance measurements of the same samples at two different $\text{Ca}_\text{T} + \text{AIII}_\text{T}$ concentrations: $10^{-3.5}$ M (upper pair) and 10^{-4} M (lower pair). The *x*-ordinate shows different equimolar ratios of $\text{Ca}_\text{T}/(\text{Ca}_\text{T} + \text{AIII}_\text{T})$. These solutions covered the full range of Ca and AIII being total Ca at the right side of the ordinate and total AIII at the left of the *x*-ordinate. The raw data from the absorbance measurements were corrected to yield zero absorbance for $\text{Ca}_\text{T}/(\text{Ca}_\text{T} + \text{AIII}_\text{T}) = 0$ (AIII only) and $\text{Ca}_\text{T}/(\text{Ca}_\text{T} + \text{AIII}_\text{T}) = 1$ (Ca only). This was attained with a linear correction for the absorbance values over the entire $\text{Ca}_\text{T}/(\text{Ca}_\text{T} + \text{AIII}_\text{T})$ range. The value at $\text{Ca}_\text{T}/(\text{Ca}_\text{T} + \text{AIII}_\text{T}) = 0$ (against a Ca blank) was the absorbance for an AIII solution with no Ca added. The value at $\text{Ca}_\text{T}/(\text{Ca}_\text{T} + \text{AIII}_\text{T}) = 1$ was set to zero. This is only one such approximation possible since the AIII_f does not vary in proportion to AIII_T. As seen in Fig. 1*A*, however, a comparison of Job plots from Ca-ISE, which are not subject to this correction, show close agreement with the absorbance data, which indicates that this approach is a valid one. Both relations produce a definite peak at $\text{Ca}_\text{T}/(\text{Ca}_\text{T} + \text{AIII}_\text{T})$ very close to 0.5. This is the expected result for binding stoichiometry of Ca^{2+} to Arsenazo of 1:1. A peak at 0.33 is expected from 2:1 binding. Values of K_D determined from measurement of Ca_f with Ca-ISE at 10 different mixtures of Ca and AIII showed a systematic increase proceeding from high AIII concentration ($K_\text{D} = 3.8 \times 10^{-6}$ M) to low AIII concentration ($K_\text{D} = 34 \times 10^{-6}$ M). Fig. 2*B* shows the relation between the changes in absorbance and Ca-AIII determined from the Ca-ISE (Ca-AIII = $\text{Ca}_\text{T} - \text{Ca}_\text{f}$). Absorbance was obtained from Cary 11 data and from the μ-spec, represented by closed and open symbols respectively. The slope of the two relations, that is, $\Delta A/\Delta$Ca-AIII $\times$ 0.5 is equal to $\Delta\epsilon_{650}$. The upper line (Cary measurements) yields a $\Delta\epsilon_{650}$ of $2.46 \times 10^4\ \text{M}^{-1}\,\text{cm}^{-1}$. This value is slightly lower than the value reported in Materials and Methods for pure AIII ($2.64 \times 10^4\ \text{M}^{-1}\,\text{cm}^{-1}$). A depression of the $\Delta\epsilon$ was consistently obtained whenever 200 mM KCl was added to the AIII solutions, as was the case in Fig. 2. Absorbance changes of AIII solutions at different ionic strengths have been reported previously (Brinley et al., 1977). The lower relation (open symbols from μ-spec) yields a $\Delta\epsilon_{650}$ of $2.18 \times 10^4\ \text{M}^{-1}\,\text{cm}^{-1}$. These data indicate that a slightly lower apparent extinction coefficient is obtained by use of the microspectrophotometer.

Fig. 3 shows Job plots for a variety of experimental conditions: different concentrations of $\text{AIII}_\text{T} + \text{Ca}_\text{T}$, different types of spectrophotometry, and for solutions with (200 mM) and without KCl. The raw data from the absorbance measurements were corrected by using a linear correction for the absorbance values as described above. Figs. 3*A* and *B* show results

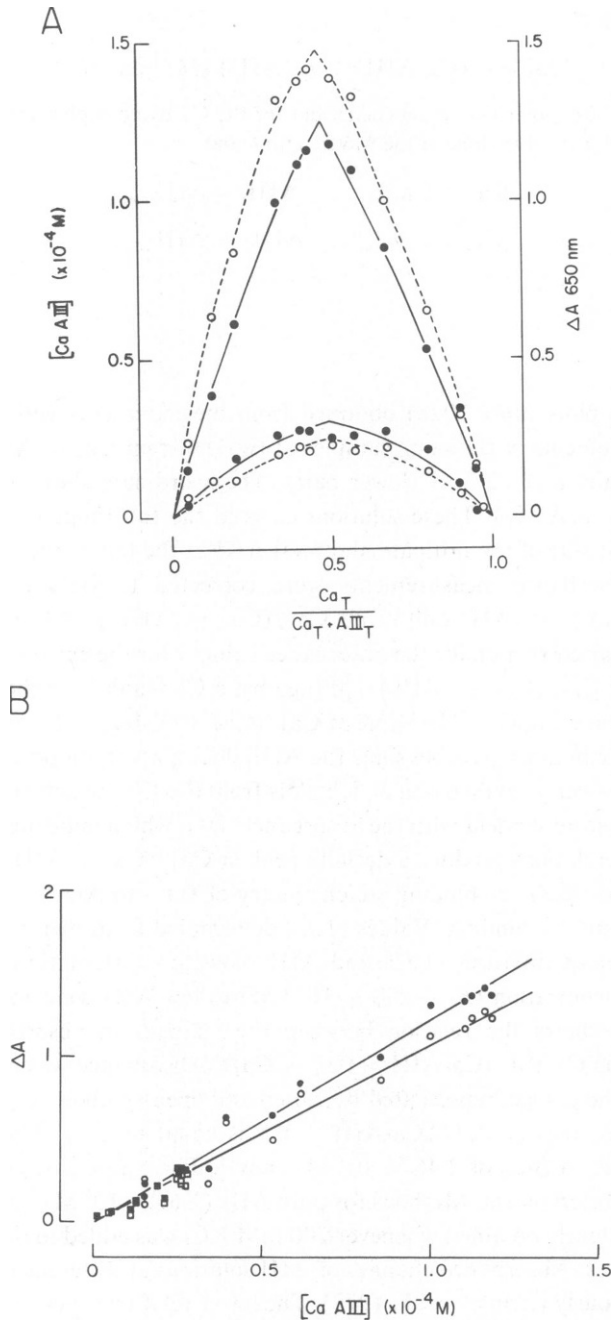

FIGURE 2 (*A*) Job plots. Abscissa: equimolar mixtures of AIII and $CaCl_2$. Ordinates: Ca-AIII concentration from Ca-ISE measurements (●) and absorbance measurements in Cary 11 (○); path length 0.5 cm. $AIII_T + Ca_T = 10^{-3.5}$ M for upper set of plots; $AIII_T + Ca_T = 10^{-4}$ M for lower set. All solutions contained 200 mM KCl, pH 7.25. (*B*) Relation between absorbance (ΔA) and CA-AIII concentration from Ca-ISE measurements; Ca-AIII = $Ca_T - Ca_f$. Filled symbols: Cary 11, 650 nm and pathlength 0.5 cm; open symbols: μ-spec, 650 vs. 720 nm and 0.01 cm; absorbance values calculated to 0.5 cm. Circles and squares represent $10^{-3.5}$ M and 10^{-4} M $AIII_T + Ca_T$, respectively. Lines from linear regression analysis.

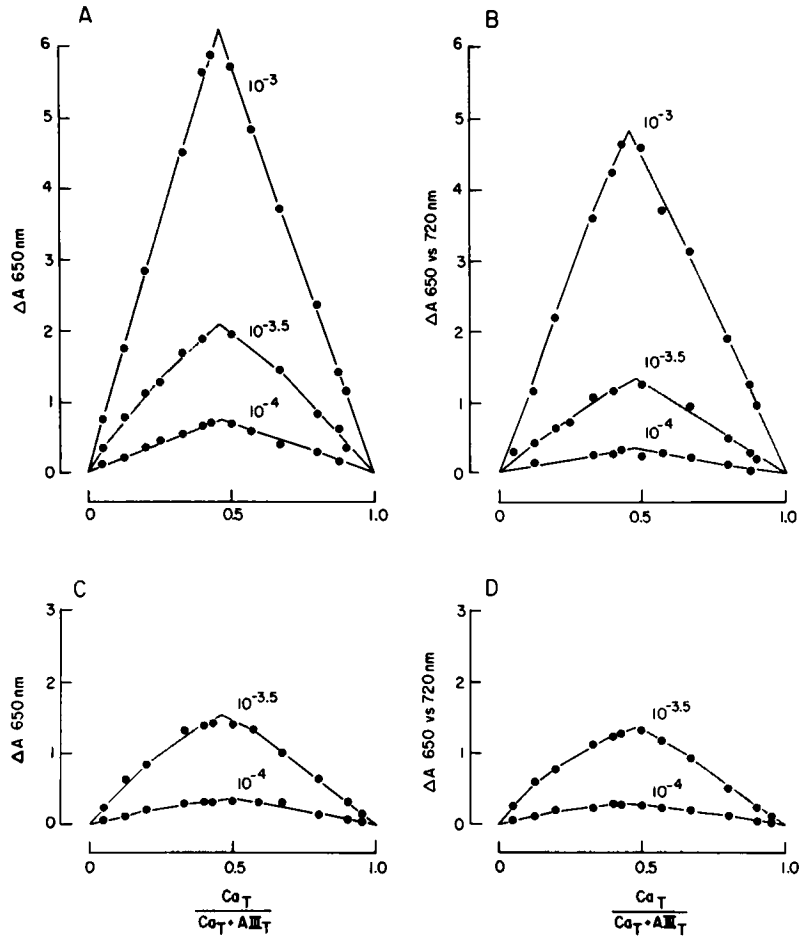

FIGURE 3 Job plots of AIII solutions of different ionic strength and $AIII_T + Ca_T$ concentration determined with different absorbance techniques. Concentrations of $AIII_T + Ca_T$ indicated next to appropriate curve. pH 7.25. (*A* and *C*) Cary 11; pathlength 0.5 cm for 10^{-4} and $10^{-3.5}$ M, 1 mm for 10^{-3} M. (*B* and *D*), μ-spec, pathlength 0.01 cm, wavelength pair 650 vs. 720 nm. *A* and *B*, 0 KCl; *C* and *D*, 200 mM KCl. All absorbance values were calculated for a 0.5 cm pathlength.

from experiments on "pure" AIII in the absence of KCl. Fig. 3*A* shows measurements obtained in the Cary 11 and Fig. 3*B*, measurements from the μ-spec. Three different concentrations of $AIII_T + Ca_T$ were used: 10^{-3}, $10^{-3.5}$ and 10^{-4} M. It can be seen that the x-value for the apex of the curves is not influenced by the kind of spectrophotometer used. The ΔA for a given ratio of $Ca_T/(Ca_T + AIII_T)$ obtained in the μ-spec may have been partly due to some uncertainty in measurement of the interfiber distance in the experimental pool of the chamber. Figs. 3*C* and *D* show experimental results in the presence of 200 mM KCl for two different concentrations of $AIII_T + Ca_T$: $10^{-3.5}$ (top) and 10^{-4} M (bottom). Fig. 3*C* shows data obtained in the Cary 11 and Fig. 3*D* data from the μ-spec. As in Figs. 3*A* and *B*, the μ-spec yields a slightly lower ΔA for a given $AIII_T + Ca_T$. The apex of the curves at both concentrations, however, is also at $Ca_T/(Ca_T + AIII_T) = 0.5$, which indicates that addition of

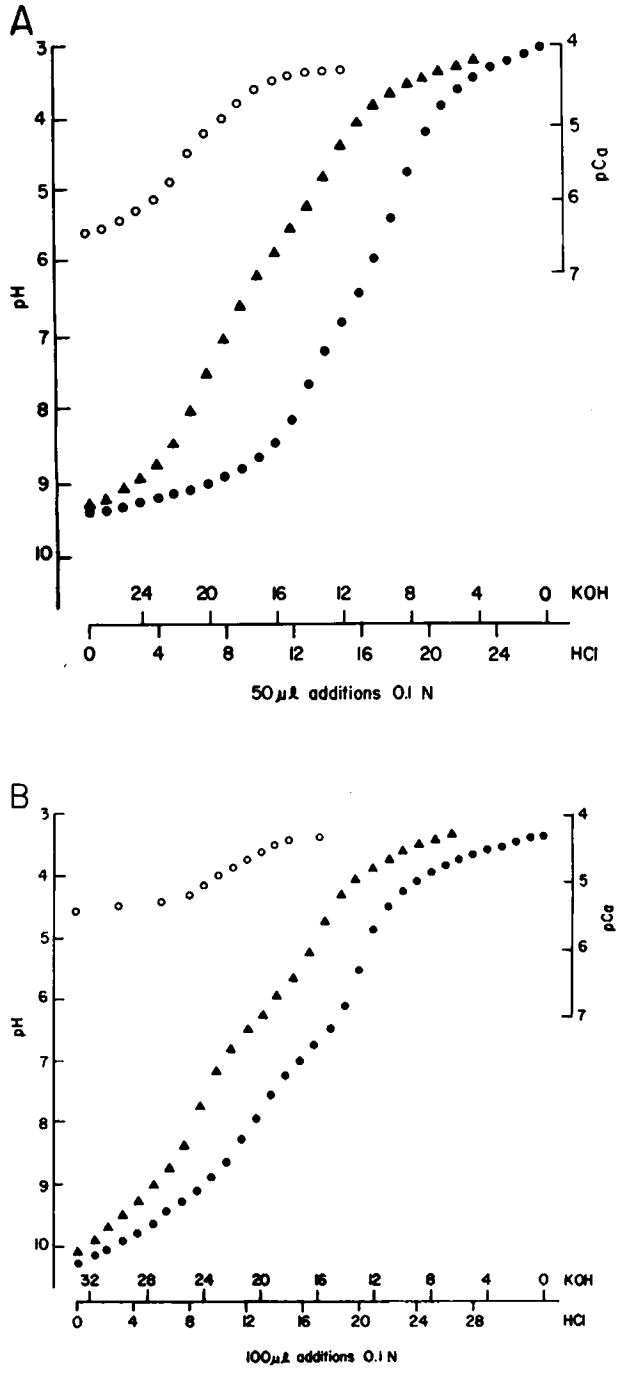

FIGURE 4 Measurement of Ca_f (open symbols) and pH (closed symbols) with Ca^{2+} and pH ISE during titration of AlII with KOH and HCl. AlII concentrations of 10^{-4} M (*A*) and $10^{-3.5}$ M (*B*) are shown. Background KCl was 200 mM. Samples were titrated with KOH in the absence of Ca^{2+} to ~pH 10 (●). $CaCl_2$ was added at this point (0.5 × [$AlII_T$]). The solutions were back-titrated to ~pH 3 with HCl (▲, ○).

KCl at these two AIII concentrations does not affect the stoichiometry of the Ca-AIII complex. But it is clear by comparing Figs. 3*A* and *C* (e.g., $10^{-3.5}$) that addition of 200 mM KCl to AIII produces a significant (~25%) reduction in absorbance.

To summarize the Job plot data, the results of Figs. 2 and 3 (whether obtained from the Ca-ISE or from absorbance data) indicate 1:1 binding stoichiometry between AIII and Ca^{2+}. This stoichiometry does not appear to be influenced by the addition of 200 mM KCl to the solutions and the results are independent of whether or not data are obtained from continuous spectra in a spectrophotometer such as the Cary Model 11 or obtained from a dual-wavelength spectrophotometer with interference filters of a greater bandwidth dispersion.

pH-Titration

Figs. 4*A* and *B* show Ca-proton exchange behavior of AIII at 10^{-4} and $10^{-3.5}$ M, respectively; 200 mM KCl was present in these solutions. In the initial part of the experiment, AIII was titrated from the acid range (left ordinate) with KOH as indicated by closed circles. The number of additions is indicated along the abscissa from right to left. The relations shown by closed circles, especially at $10^{-3.5}$ M AIII, show that AIII buffers pH most effectively at ~ pH 4, 6.8, and 9.5. Addition of $CaCl_2$ (one-half the AIII concentration) at the end of titration with KOH decreased the pH of the solution at both AIII concentrations. Upon back-titration of the pH of the solution with HCl (triangles), it is evident that fewer additions were necessary to attain the same pH. This indicates that Ca^{2+} renders the AIII molecule less potent in buffering protons. Free Ca^{2+} (Ca-ISE) was measured during back-titration after addition of the $CaCl_2$. The values in pCa (-log[Ca]) are shown on the right ordinate. Both show a gradual rise in Ca_f during the first few additions and a much more rapid increase in Ca_f over the mid-pH range. Thereafter, the Ca_f values approach a plateau. The Ca_f values obtained at low pH indicate that a substantial amount of Ca^{2+} remains bound to the AIII. Values for K_D were calculated from the known concentration of AIII, the total amount of Ca^{2+} added, the amount of Ca^{2+} as an impurity in AIII, and measurement of free Ca^{2+} with the ISE (Eq. 2). They show a distinct pH dependence (see Table I). For example, at $10^{-3.5}$ M AIII, K_D on the order

TABLE I
K_D FOR THE REACTION BETWEEN AIII AND Ca^{2+} AT DIFFERENT AIII CONCENTRATIONS AND pH

	K_D (μM)	
pH	10^{-4} M [AIII]	$10^{-3.5}$ M [AIII]
3.0	389	98
4.0	389	98
5.0	389	102
6.0	137	41.0
7.0	20.3	13.1
8.0	5.2	6.8
9.0	0.5	5.5
10.0	0.3	4.5

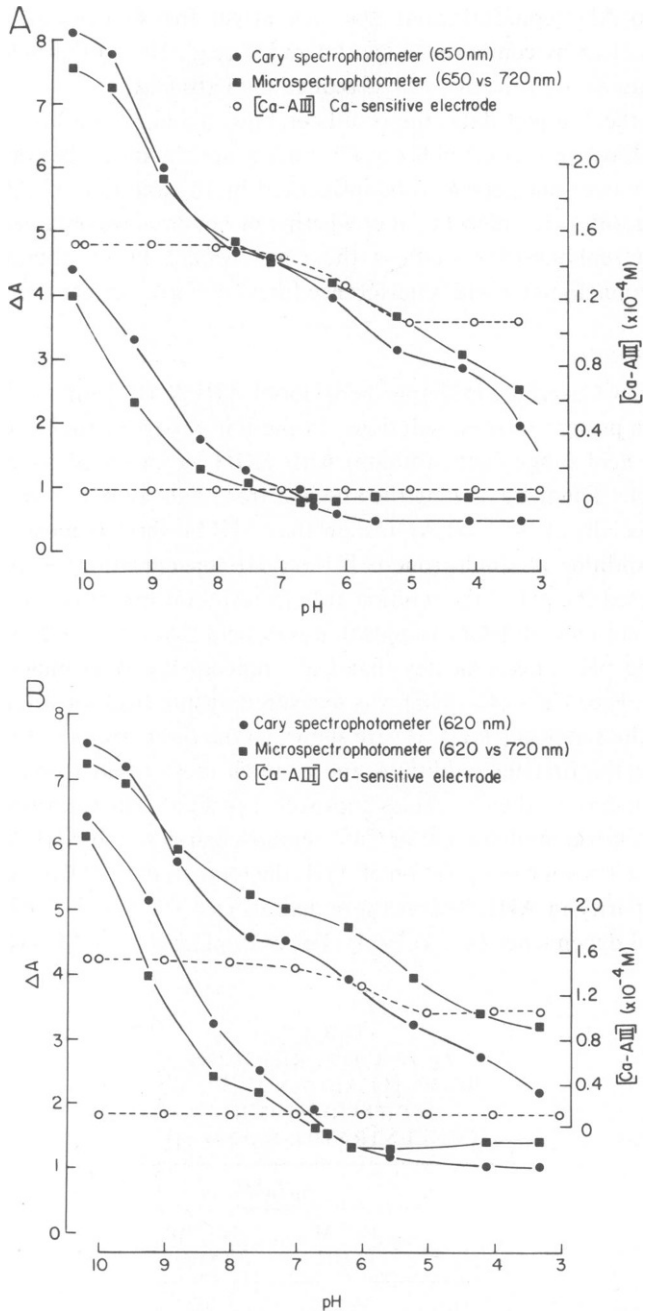

FIGURE 5 Absorbance changes (filled symbols) and Ca-AIII determined with Ca-ISE (open symbols) vs. pH for a $10^{-3.5}$ M AIII solution. The lower relations are for AIII alone, whereas the upper set of relations are for AIII with 1.5×10^{-4} M $CaCl_2$ added. All solutions contained 200 mM KCl. Absorbance measurements were made against water in Cary 11 (●) and μ-spec (■) at 650 nm (*A*) and at 620 nm (*B*). Experimental pathlengths were 0.1 cm and 0.01 cm for the Cary 11 and μ-spec, respectively. Absorbance values shown were calculated to 1-cm pathlength. Ca-AIII (Ca_T – Ca_f) determined from Ca_f measurements with Ca-ISE.

of 5 μM are obtained at high pH, whereas in the midrange around pH 7, values of ~13 μM are obtained. At low pH in the range pH 4–3, values of ~100 μM are obtained. These values obtained from Ca-ISE measurements are in quite close agreement with values obtained by Chiu and Haynes (1980).

Fig. 5 shows plots of absorbance changes vs. pH from the same $10^{-3.5}$ M AIII solution described in Fig. 4. During additions of KOH or HCl, absorbance measurements of aliquots of the solutions were made in the Cary 11 and the μ-spec. Spectra were obtained between 500 and 750 nm in the Cary 11; absorbance changes (left ordinate) are shown for 650 nm in Fig. 5*A* and 620 nm in Fig. 5*B*, by the solid circles. Results from the μ-spec at the wavelength pairs 650–720 nm and 620–720 nm are shown by solid squares in Figs. 5*A* and *B*, respectively. The right ordinate shows the Ca-AIII calculated from the free Ca^{2+} measurements obtained with the Ca-ISE. These data are represented by the open symbols. The two sets of data shown in the lower part of Figs. 5*A* and *B* are for measurements of $10^{-3.5}$ M AIII, with no Ca^{2+} added. It can be observed that the Ca-ISE measurements showed very little change in Ca-AIII between pH 3 and 10. At low pH, between 3 and 6, absorbance measurements (ΔA) at 650 and 620 nm also showed little change. Between pH 6 and 8, however, there was an increase in absorbance as the pH was increased. At ~pH 8, there was a very large increase in absorbance as the pH was increased. The pH dependency over the midrange of pH, that is, between 5.5 and ~ 8, was greater at 620 than at 650 nm and the slope was still steeper between pH 8 and 10. With Ca^{2+} added to the solutions (top sets of relations), the Ca-ISE indicated little change in Ca-AIII between pH 3 and 5. On the other hand, the absorbance at 650 and 620 nm increased with pH over this same range. Between pH 5 and ~ 8, the Ca-ISE indicated an increase in Ca-ligand formation. Absorbance changes in both the Cary and the μ-spec paralleled the Ca-ISE. Beyond pH 8, Ca-ligand changed very little, but the AIII showed a strongly pH-dependent absorbance increase at both 650 and 620 nm roughly paralleling the low Ca solutions. Comparison of the Ca-ISE results with those obtained from absorbance measurements indicates a close correlation of absorbance changes with Ca-AIII formation over the midrange of pH values, i.e., between pH 5 and 8. Beyond the extremes of this range of pH, AIII shows strongly pH-dependent absorbance changes independent of Ca-AIII formation. To facilitate a comparison of Ca-AIII from absorbance data with the electrode data, the right ordinate was located and scaled according to the relation

$$\Delta A^{7.25} = \epsilon_{\text{AIII}}^{7.25} \times 10^{-3.5} + [\text{Ca-AIII}] \times \Delta\epsilon_{(\text{Ca-AIII})}^{7.25}, \tag{7}$$

where $\epsilon_{\text{AIII}}^{7.25}$ and $\Delta\epsilon_{(\text{Ca-AIII})}^{7.25}$ are values obtained from Fig. 1.

Calcium Additions at Different Ionic Strength

Several experiments were conducted to evaluate the effect of different concentrations of KCl on AIII absorbance and Ca_f changes during titration with $CaCl_2$. During the $CaCl_2$ additions, absorbance changes were measured in both the Cary 11 and the μ-spec. Results were essentially the same. Results from the Cary 11 are shown in Fig. 6, which are from AIII solutions containing no KCl (*A*) and 200 mM KCl (*B*). Absorbance changes are represented by closed symbols.

Ca-AIII, calculated from Ca_T and the Ca_f measured with ISE, are represented by open symbols. AIII concentrations were 10^{-3} M (diamonds), $10^{-3.5}$ M (triangles), 10^{-4} M

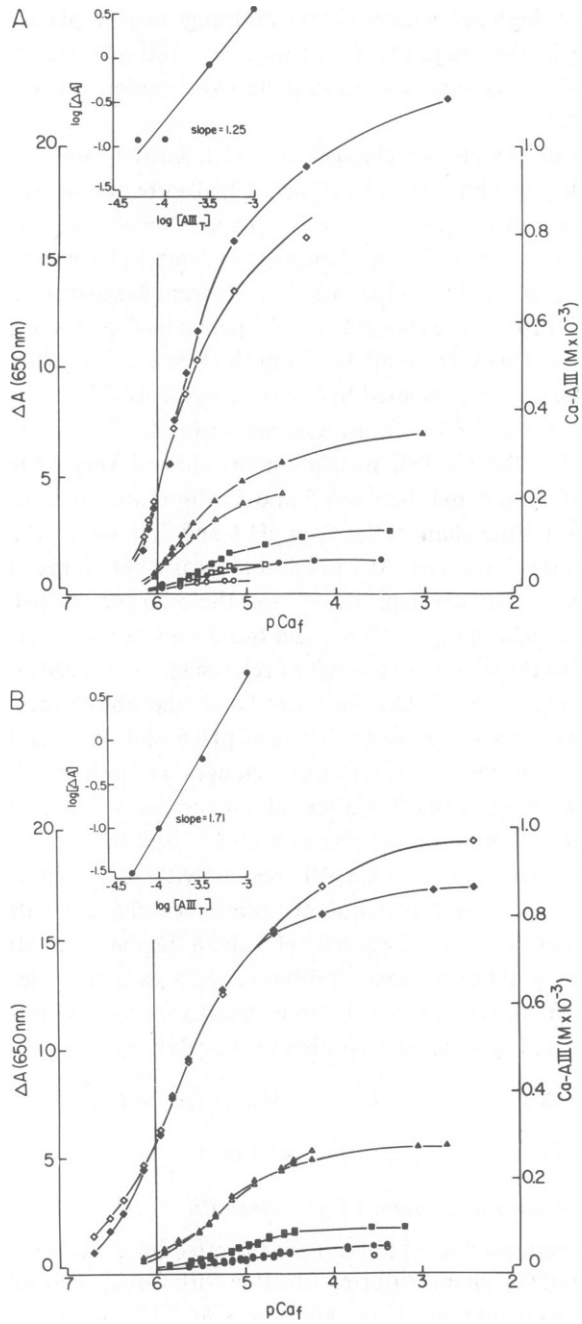

FIGURE 6 $CaCl_2$ titration experiments showing absorbance changes (ΔA-filled symbols) and Ca-AIII concentration changes (open symbols) vs. pCa_f ($-\log Ca_f$). Ca-AIII = $Ca_T - Ca_f$, determined from Ca_f measurements with Ca-ISE. (*A*) AIII solutions containing 1 mM Hepes buffer. $\Delta\epsilon^{650} = 2.5 \times 10^4\ M^{-1}\ cm^{-1}$. (*B*) AIII solutions containing 1 mM Hepes + 200 mM KCl. $\Delta\epsilon^{650} = 1.9 \times 10^4\ M^{-1}\ cm^{-1}$. ○●, $10^{-4.3}$ M AIII; □■, 10^{-4} M AIII; △▲, $10^{-3.5}$ M AIII; ◇◆, 10^{-3} M AIII. Experimental pathlengths 0.1, 0.5 and 1 cm; absorbance data shown were calculated to 1 cm pathlength. *Insets:* log ΔA vs. log $AIII_T$ relation at $Ca_f = 1 \times 10^{-6}$ M, as indicated by vertical line in main graphs.

(squares), and $10^{-4.3}$ M (circles). In these experiments, the "zero" calcium absorption spectrum was established by adding EGTA (0.1–0.5 mM) to one sample of the test solution. The Ca^{2+} impurity for AIII was a mean value from the four AIII solutions, based on absorbance data. To saturate the AIII solutions, $CaCl_2$, 5–10 times the AIII concentration, was added to the test solutions. These large additions were also used to establish a calibration point for the Ca-ISE. The relation between log ΔA and log [AIII] (cf. Gorman and Thomas, 1978) was obtained from these curves by reading vertically across the curves at a certain pCa, as indicated by the solid vertical line. One such plot for each experiment at $Ca_f = 10^{-6}$ M is shown in the insets. It is evident that the addition of 200 mM KCl increases the slope of this relation from 1.25 to 1.71. The AIII concentrations in these plots have not been corrected for the formation of Ca-AIII and are used for comparison only.

Another approach to the analysis of the calcium addition experiments is to assume n Ca^{2+} reacting with an AIII molecule and to rearrange the equilibrium equation according to Hill (1910):

$$\log \frac{\Delta A}{\Delta A_{max} - \Delta A} = n_H \log Ca_f + \log \frac{1}{K_D}. \tag{8}$$

There are several advantages of using this approach. The maximum Ca-AIII is known ($AIII_T$). Ca_f is directly measurable with the Ca-ISE. The slope of the plot obtained is independent of K_D, which can be particularly important if K_D is a function of the AIII concentration. Fig. 7 shows relations between log ($\Delta A/\Delta A_{max} - \Delta A$) and log Ca_f for the data of Fig. 6 where Figs. 7*A* and *B* are for 0 and 200 mM KCl, respectively. In Fig. 7*A* (0 KCl), the data from the four concentrations of AIII seem to yield essentially the same relation. A linear regression analysis of all points yields a line with a slope of 1.02, which indicates a 1:1

TABLE II
EQUILIBRIUM BINDING CONSTANTS FOR THE AIII-Ca^{2+} REACTION AT DIFFERENT AIII AND KCl CONCENTRATIONS

KCl (mM)	$AIII_T$ (M)				
	Constants	$10^{-4.3}$	10^{-4}	$10^{-3.5}$	10^{-3}
0	K_D, μM*	4.17	5.13	4.37	3.47
	$\bar{K}_D$, μM‡	3.90	5.51	5.65	5.62
	n_H	1.27	1.14	0.83	0.83
	n_S	1.00	1.00	0.82	0.84
10	K_D, μM*	6.90	4.60	2.81	2.10
	$\bar{K}_D$, μM‡	7.04	5.71	2.79	3.01
	n_H	1.19	1.50	1.37	1.19
	n_S	1.10	1.10	1.06	0.99
200	K_D, μM*	14.1	8.13	5.60	2.00
	$\bar{K}_D$, μM‡	15.5	8.84	6.57	2.41
	n_H	1.27	1.21	1.07	1.00
	n_S	0.95	0.95	1.00	1.00

*K_D obtained from intersection of a line between points where $\Delta A/(\Delta A_{max} - \Delta A) = 0$ (cf. Fig. 7).
‡K_D = ($Ca_f \times AIII_f$/Ca-AIII); K_D = average value from all $CaCl_2$ additions.

relationship between Ca^{2+} and AIII. In Fig. 7*B*, the four concentrations of AIII yielded four relations that parallel one another quite closely; see Table II. There was a slight curvature in the relation that is especially apparent in the 10^{-3} M relation. This is most likely due to some inaccuracy in reading the low Ca_f with the Ca-ISE. A linear regression analysis of the data at each concentration yielded the n_H values reported in Table II. The lines are displaced along the *x*-axis, which indicates a systematic change of K_D with AIII concentration. Assuming $n_H = 1$, $Ca_f = K_D$ when $\log \Delta A/(\Delta A_{max} - \Delta A) = 0$ (cf. Eq. 8). In Fig. 7*B*, the largest K_D was obtained for $10^{-4.3}$ M AIII (14.0×10^{-6} M), whereas a K_D of 2.5×10^{-6} M was obtained for 10^{-3} M AIII. With Ca_f, $AIII_f$, and Ca-AIII obtained from electrode and absorbance data, a

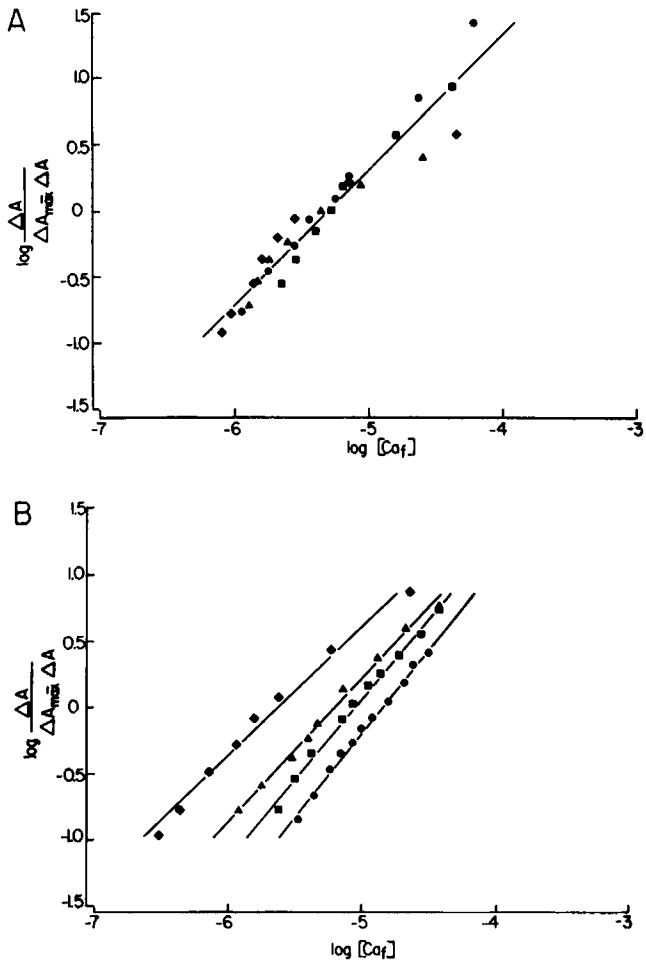

FIGURE 7 Hill plot for data in Fig. 6; see text for analytical treatment. (*A*) AIII solutions with 1 mM Hepes only (pH 7.25). A linear regression analysis of all points obtained during $CaCl_2$ addition that were nonsaturating yielded a line with a slope of 1.02. The corresponding K_D value was 4.8×10^{-6} M, i.e., $K_D = Ca_f$ at $\Delta A/(\Delta A_{max} - \Delta A) = 0$ (see Eq. 8). (*B*) AIII solutions with 1 mM Hepes + 200 mM KCl (pH 7.25). Linear regression analysis yielded lines for the different AIII concentrations with similar slopes but with different K_D values: $10^{-4.3}$ AIII: 14.0×10^{-6} M; 10^{-4} AIII: 8.8×10^{-6} M; $10^{-3.5}$ AIII: 6.5×10^{-6} M; 10^{-3} AIII: 2.5×10^{-6} M.

mean K_D can be calculated for the different AIII concentrations. These $\overline{K}_D$ correspond closely to the values arrived at graphically from Fig. 7, as shown in Table II, which summarizes data from 0, 10, and 200 mM KCl.

A Scatchard analysis was conducted on the same data (not illustrated). This analysis provides the number of independent binding sites for Ca^{2+} on the AIII molecule (n_S) from the following expression:

$$\frac{\text{Ca-AIII}}{\text{Ca}_f} = -\frac{1}{K_D}(\text{Ca-AIII} - n_S \cdot \text{AIII}_T). \tag{9}$$

In this case, the slope of the relation gives the reciprocal value of K_D and the x-intercept represents $n_S \cdot \text{AIII}_T$. The Ca-AIII concentration was calculated from the absorbance measurements and the Ca_f was obtained from Ca-ISE. The mean ± SD value of n_S for the four AIII concentrations was 0.91 ± 0.10 for the zero KCl solutions and 0.99 ± 0.04 for the 200-mM KCl solutions. The K_D values calculated from the slopes of the relations of the 200-mM solutions increased as AIII was reduced, whereas they were essentially constant in the zero KCl solutions. This is consistent with the Hill analysis shown in Fig. 7.

Absorbance Behavior of AIII in Different Ca^{2+} Buffer Systems

Several studies using the Gorman and Thomas (1978) paradigm were conducted to determine whether their results could be confirmed and to evaluate whether the results are dependent upon the type of buffer system used. It is worth noting that Ahmed et al. (1980) were unable to confirm the Gorman and Thomas finding that a log ΔA-log AIII plot yields a slope close to 2. Log-log relations of the absorbance changes vs. AIII_T are shown in Fig. 8. These solutions contained 200 mM KCl, 10 mM EGTA, 10 mM Hepes, and 7.5 mM $CaCl_2$ (pH 7.25). Figs.

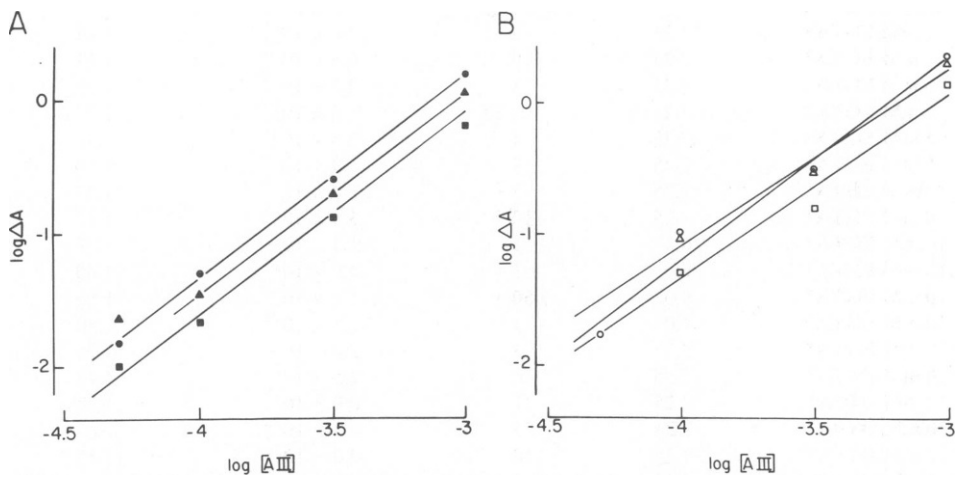

FIGURE 8 Log ΔA-log AIII relations obtained from absorbance measurements in Cary 11 (A) and μ-spec (B). Pathlengths for Cary 11 were 0.1, 0.5 and 1.0 cm for 10^{-3}, $10^{-3.5}$, and 10^{-4} M AIII, respectively. Pathlength for μ-spec was 0.01 cm. Values of absorbance shown are calculated for a 1-cm pathlength. Solutions contained 200 mM KCl, 10 mM EGTA, 7.5 mM $CaCl_2$ ($Ca_f = 3\ K_D^{EGTA}$), and 10 mM Hepes (pH 7.25). The blank contained all constituents except the 7.5 mM $CaCl_2$. All lines calculated from linear regression analysis (cf. Table III).

TABLE III
SLOPES OF THE RELATION LOG ΔA VS. LOG[AIII] FROM FIG. 8

	Slope	
λ (*nm*)	Cary 11	μ-spec
650 (●,○)	1.56	1.53
620 (■,□)	1.55	1.42
600 (▲,△)	1.54	1.34

8*A* and *B* show results obtained from the Cary 11 and μ-spec, respectively. Owing to the low Ca_f in these experiments ($Ca_f = 3K_D^{EGTA} = 1.98 \times 10^{-7}$ M; K_D from Bjerrum et al., 1957; Owen, 1976), $AIII_T$ was considered to be the same as $AIII_f$ (*x*-axis). Results at three different wavelengths from the Cary 11 are presented in Fig. 8*A*: 650, 620, and 600 nm. The slope of the relations in Fig. 8*A* are essentially the same, the values of the slope being ~1.55. Results from the μ-spec (Fig. 8*B*) were similar for 620 and 600 vs. 720 nm (squares and triangles); values for the slopes of the relations were 1.42 and 1.34, respectively. The value at 650 nm (open circles) had a steeper slope, 1.53. These results are summarized in Table III.

Following the same protocol as the experiment in Fig. 8, we conducted a number of other

TABLE IV
SLOPE OF LOG ΔA-LOG AIII RELATIONS FOR DIFFERENT Ca-BUFFER SYSTEMS

Buffer system	pH	ΔCa_f	ΔCa_f	Slope log ΔA/log AIII
Experiment		($n \cdot K_D$)	(M)	
1 mM EGTA*	7.25	3	2.0×10^{-7}	1.63
1 mM EGTA*	7.25	10	6.6×10^{-7}	1.57
5 mM EGTA*	7.25	3	2.0×10^{-7}	1.83
5 mM EGTA‡	7.25	2.33	1.5×10^{-7}	1.75
5 mM EGTA‡	7.25	4	2.6×10^{-7}	1.74
5 mM EGTA‡	7.25	9	5.9×10^{-7}	1.70
10 mM EGTA*	7.25	3	2.0×10^{-7}	1.57
10 mM EGTA*	7.25	10	6.6×10^{-7}	1.48
10 mM EGTA*	6.0	1	1.3×10^{-5}	1.57
10 mM EGTA*	6.0	3	4.0×10^{-5}	1.60
10 mM EGTA*	8.0	~50	1.1×10^{-7}	1.52
10 mM EGTA*	8.0	~15	3.3×10^{-8}	1.40
30 mM EGTA*	7.25	3	2.0×10^{-7}	1.70
10 mM EDTA*	7.25	10	2.5×10^{-7}	1.79
10 mM DTPA*	7.25	1	0.9×10^{-7}	1.78
10 mM DTPA*	7.25	5	4.5×10^{-6}	1.65
10 mM DTPA*	7.25	10	9.0×10^{-6}	1.59
10 mM NTA*	7.25	0.1	1.45×10^{-5}	1.34

$K_D^{EDTA} = 2.5 \times 10^{-8}$ M (Ringbom, 1963). $K_D^{EGTA} = 6.6 \times 10^{-8}$ M (Bjerrum et al., 1957; Owen, 1976). K_D^{EGTA} (pH 8) = 2.2×10^{-9} M (Ringbom, 1963). K_D^{EGTA} (pH 6) = 1.3×10^{-5} M (Ringbom, 1963). $K_D^{DTPA} = 0.9 \times 10^{-6}$ M (our measurements). $K_D^{NTA} = 1.45 \times 10^{-4}$ M (Ringbom, 1963).

*200 mM KCl, 10 mM Hepes. Mean slope at pH 7.25 ($n = 11$): 1.63 ± 0.14.

‡350 mM KCl, 150 mM MOPS; same protocol as Ahmed et al. (1980).

experiments using different Ca^{2+}-buffering systems to maintain Ca_f at different fixed levels. In these experiments, the Cary 11 spectrophotometer was used to measure absorbances. Results from this series of experiments are found in Table IV. Four different Ca^{2+} buffers were used: EDTA, EGTA, diethylenetriamine pentaacetic acid (DTPA), and nitrolotriacetic acid (NTA). When high Ca_f concentrations were attained, log $AIII_f$ rather than log $AIII_T$ was plotted, because a substantial part of the AIII is bound to Ca^{2+}. In those cases where either the K_D of the buffer approached that of AIII (DTPA and NTA) or the concentrations of the buffer approached that of AIII, the Ca_f was recalculated from a two-buffer system with a cubic equation. The Ca_f value calculated was used to correct the absorption to a level corresponding to a Ca_f that would have been obtained if the Ca-buffer alone had set the Ca_f level. For example, with 10 nM NTA (experiment 18), the slope obtained without any correction was 1.06. With the above mentioned corrections, the slope was 1.34.

The slopes of the log-log relations obtained show no apparent systematic changes. The mean value for the slope of the relations for all buffers with 200 mM KCl is 1.63. In a few experiments (EGTA 10mM, experiments 9–12) the pH was varied, the values for the slope were essentially unchanged.

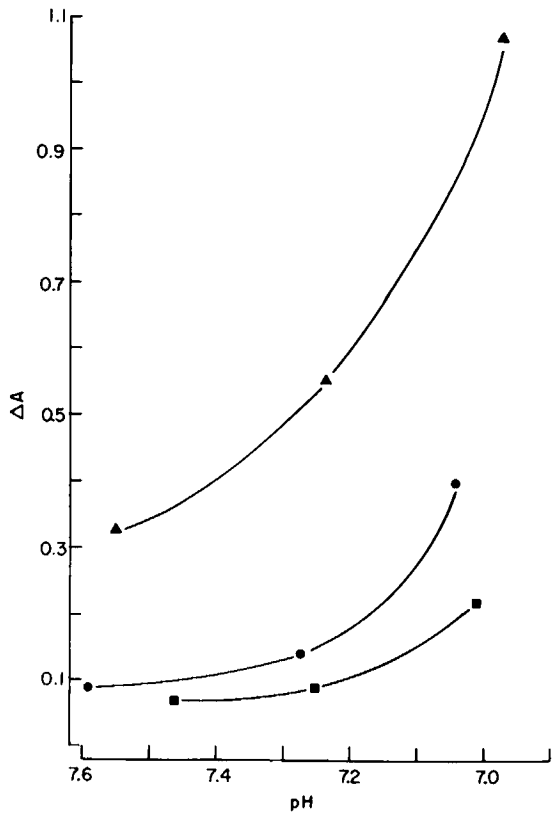

FIGURE 9 Absorbance differences vs. pH of AIII-Ca/EGTA solutions; 10^{-3} M AIII (▲), $10^{-3.5}$ M AIII (●), and 10^{-4} M AIII (■). Each AIII solution contained 200 mM KCl, 10 mM EGTA, 7.5 mM $CaCl_2$ ($Ca_f = 3\ K_D^{EGTA}$), and 10 mM Hepes. Blank contained all constituents except $CaCl_2$. All measurements made in Cary 11 at 650 nm. Pathlength 1 cm.

In general, this type of analysis produces slopes considerably greater than would be anticipated on the basis of the Job plots, Hill plots, or Scatchard analysis presented earlier. Fig. 10 in Discussion reconciles this paradox.

Fig. 9 shows absorbance changes for AIII solutions containing 200 mM KCl, 10 mM EGTA, 10 mM Hepes, and 7.5 mM total $CaCl_2$ at various pH values in the physiological range. AIII concentrations were 10^{-4} M (■), $10^{-3.5}$ M (●) and 10^{-3} M (▲). These relations show that in a complex medium containing another Ca^{2+} ligand, i.e., EGTA, the absorbance changes of AIII may increase rather than decrease as the acidity of the medium is increased. This is to be expected when the K_D of the other ligand is significantly smaller than the K_D of AIII. In this case, as the pH of the medium was changed, EGTA yielded Ca^{2+} to the AIII molecule, which increased in absorbance, even though as shown previously (Fig. 5) the inherent property of AIII shows a decrease in absorbance with the same change in pH. These measurements of AIII allow an independent calculation for the K_D of EGTA. If we assume that K_D-AIII equals 10^{-5} M at pH 7.3, then a free Ca^{2+} value of 1.85×10^{-7} M is calculated from the absorbance change. This free Ca^{2+} value translates into a K_D-EGTA of 0.67×10^{-7} M, which is very close to that obtained previously from Ca^{2+} microelectrode measurements at the same pH of 7.3 (Owen, 1976; see also Bjerrum et al., 1957). The same calculation for pH 7.0 produced a value of 1.62×10^{-7} M.

DISCUSSION

A variety of techniques was used to evaluate four fundamental problems associated with the use of AIII as an intracellular Ca^{2+} indicator: (*a*) the binding stoichiometry of AIII and Ca^{2+}, (*b*) variation of the apparent dissociation constant (K_D) of AIII under a variety of conditions that are pertinent to application of AIII to physiological problems, (*c*) the influence of pH, and (*d*) different spectrophotometric techniques. Thomas' (1979) investigation of AIII is one of the few detailed studies conducted with a microspectrophotometer. His conclusions also stand in contradistinction to most others in that they indicate a 2:1 binding stoichiometry for AIII:Ca. Ahmed et al. (1980) suggested that one possible reason they could not replicate Thomas' result might have been their different absorption measurement techniques. Results from the present investigation indicate that dual-wavelength spectrophotometry provides essentially the same results as selected absorbance values from a full wavelength scan of the samples. This presupposes that a given wavelength from absorption spectra is compared directly with the specific peak transmission of the interference filter.

The pH titration experiment (cf. Fig. 5) shows that protons exert two basic effects on AIII absorbance changes. Between ~ pH 6 and 8, absorbance changes seem to follow Ca-AIII formation quite closely. This is most clearly seen in the upper graphs in Figs. 5*A* and *B*. This change in Ca-AIII formation parallels the change in K_D at different pH, as seen in Table I. At the extremes of pH, i.e., above pH 8 and below pH 6 there are absorbance changes which are independent of Ca-AIII formation. These changes are also more obvious in the high Ca_T (upper graphs). This behavior of the AIII molecule can be expressed in terms of changes in extinction coefficient at these pH extremes. In the physiological range of pH, the pH dependence of AIII can be obtained from the slope of the *A*-pH curve having the units M^{-1} cm^{-1} pH^{-1}.

The absorbance changes of AIII are thus composed of two parts. One is determined by

Ca-AIII formation and the other determined by pH changes. The pH dependence is more pronounced at 620 than at 650 nm. This is in agreement with the results from Ogan and Simons (1979), who showed that the most pH-sensitive wavelength was close to 605 nm.

Different methods used to evaluate the binding stoichiometry of AIII-Ca produced a paradox initially. That is, analyses based on equimolar mixtures of AIII and Ca (Job analysis) or Ca additions at a given concentration of AIII produced results indicating 1:1 complexation. On the other hand, when the analysis was conducted across AIII concentrations, i.e., log ΔA or log $[Ca_T - Ca_f]$ from electrode experiments vs. log [AIII], slopes >1 were always obtained. This was the case, even though a variety of Ca buffers were used as shown in Table IV. This was not easily reconciled until we considered the effect of AIII concentration and ionic strength on K_D.

From the Hill plots (Fig. 7) and from calculations of K_D from Ca_f, $AIII_f$, and Ca-AIII (Eq. 2), it is evident that K_D varies with the concentration of AIII and the potassium chloride in the test solutions. This raises the question whether this can explain the steep slopes obtained in the log ΔA vs. log AIII plots (cf. Table IV). By plotting K_D as a function of $AIII_T$ in a log-log diagram, reasonably straight lines were obtained as shown in Fig. 10, where ●, ▲, and ■ represent AIII solutions containing 200, 10, and 0 mM KCl, respectively. This indicates that K_D can be expressed as a power function of $AIII_T$, i.e., $K_D = a \times [AIII_T]^m$, where a is an arbitrary constant and m is the slope of the relation and depends on the KCl concentration, as shown in Fig. 10. If the expression for K_D is substituted into the equilibrium equation (Eq. 1) and solved for Ca-AIII we get

$$\text{Ca-AIII} = \frac{AIII_f}{a \cdot [AIII_T]^m} \cdot Ca_f.$$

Assuming a constant Ca_f value and $AIII_f = AIII_T$ (for small Ca_f values), we get

$$\text{Ca-AIII} = AIII_T^{(1-m)} \cdot \left(\frac{Ca_f}{a}\right). \tag{11}$$

From Fig. 10, an m value of -0.62 is obtained for 200 mM KCl, which yields an exponent of 1.62 for Eq. 11. This is in excellent agreement with the mean value of m for the different

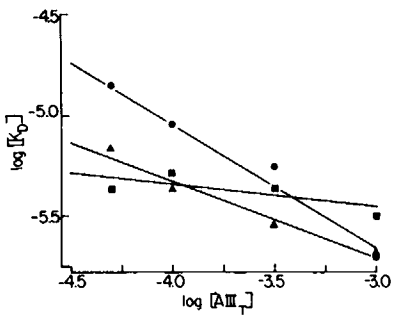

FIGURE 10 Plots of log K_D vs. log $AIII_T$ for different KCl concentrations: 0-KCl (■), 10 mM KCl (▲), 200 mM KCl (●); lines from linear regression analysis. 1 mM Hepes added to all solutions (pH 7.25). K_D for the different AIII concentrations was obtained from intersection of line between experimental points in Fig. 7 where log $(\Delta A/\Delta A_{max} - \Delta A) = 0$. See footnote (*) in Table II.

Ca-buffer experiments containing 200 mM KCl (cf. Table IV). The m value for the 10-mM KCl solution is -0.39 and for the zero KCl -0.10, which indicates decreasing variability of K_D as the KCl is reduced. Whether the potassium per se is responsible for this change in K_D, or whether it is due to a general ionic strength effect, is not clear. There is some indication (Ogan and Simons, 1979) that cations can exert differential effects on AIII absorbance.

Thus, we have obtained essentially the same experimental result as Thomas (1979), i.e., that the log ΔA-log AIII relation is steep at high ionic strength, but we are at variance with his conclusion that this indicates 2:1 binding stoichiometry. This particular plot rather indicates that the K_D of AIII varies with [AIII] as well as ionic strength. There was qualitative indication that the binding sites on AIII could be different, depending on the ionic strength of the solution. That is, titration of AIII solutions at weak ionic strength releases protons to the medium, as is revealed by a pH electrode, and this effect is small by comparison at high ionic strength.

Received for publication 23 January 1981 and in revised form 14 April 1981.

REFERENCES

Ahmed, Z., and J. A. Connor. 1980. Intracellular pH changes induced by calcium influx during electrical activity in molluscan neurons. *J. Gen. Physiol.* 75:403–426.

Ahmed, Z., L. Kragie, and J. A. Connor. 1980. Stoichiometry and apparent dissociation constant of the calcium-Arsenazo III reaction under physiological conditions. *Biophys. J.* 32:907–920.

Bjerrum, J., G. Schwartzenbach and L. G. Sillen. 1957. Stability Constants. Part 1. *In* Organic Ligands. The Chemical Society, London.

Brinley, F. J., T. Tiffert, A. Scarpa, and L. J. Mullins. 1977. Intracellular calcium buffering capacity in isolated squid axons. *J. Gen. Physiol.* 70:355–384.

Brown, H. Mack, J. P. Pemberton, and J. Owen. 1976. A calcium-sensitive microelectrode suitable for intracellular measurement of calcium (II) activity. *Anal. Chim. Acta.* 85:261–276.

Brown, H. Mack, and B. Rydqvist. 1980*a*. Ca^{2+} microelectrode and Arsenazo III absorbance changes as a consequence of injected Ca^{2+} in *Balanus* photoreceptors. *Fed. Proc.* 39:2137.

Brown, H. Mack, and B. Rydqvist. 1980*b*. Changes of intracellular Ca^{2+} in *Balanus* photoreceptors probed with Ca^{2+} microelectrodes and Arsenazo III. *Proc. Int. Union Physiol. Sci.* 14:339.

Brown, J. E., P. K. Brown, and L. H. Pinto. 1977. Detection of light-induced change of intracellular ionized calcium concentration in *Limulus* ventral photoreceptors using Arsenazo III. *J. Physiol.* 267:299–320.

Buděšinský, B. 1969*a*. Acidity of several chromotropic acid AZO derivatives. Talanta 16:1277–1288.

Buděšinský, B. 1969*b*. Monoarylazo and bis(arylazo) derivatives of chromotropic acid as photometric reagents. *In* Chelates of Analytical Chemistry. Vol. 2. H. A. Flaschka and A. J. Barnard, editors. Marcel Dekker, Inc., New York.

Chance, B. 1972. Principles of differential spectrophotometry with special reference to the dual-wavelength method. Methods Enzymol. 24:322–335.

Chiu, V. C. K., and D. Haynes. 1980. The pH dependence and the binding equilibria of the calcium indicator-AIII. *Membr. Biochem.* 3:169–183.

Gorman, A. L. F., and M. V. Thomas, 1978. Changes in the intracellular concentration of free calcium ions in a pacemaker neuron, measured with the metallochromic indicator dye Arsenazo III. *J. Physiol.* 275:357–376.

Gratzer, W. B., and G. H. Beaven. 1977. Use of the metal-ion indicator, Arsenazo III, in the measurement of calcium binding. *Anal. Biochem.* 81:118–129.

Hill, A. V. 1910. A new mathematical treatment of changes of ionic concentration in muscle and nerve under the action of electric currents, with a theory as to their mode of excitation. *J. Physiol.* 40:190–324.

Job, P. 1928. Reserches sur la formation de complexes minéraux en solution et sur leur stabilité. *Ann. Chim.* 9:113–203.

Michaylova, V., and P. Ilkova. 1971. Photometric determination of micro amounts of calcium with Arsenazo III. *Anal. Chim. Acta.* 53:194–198.

Ogan, K., and E. Simons. 1979. The influence of pH on Arsenazo III. *Anal. Biochem.* 96:70–76.

Owen, J. D. 1976. The determination of the stability constant for calcium-EGTA. *Biochim. Biophys. Acta.* 451:321–325.

Owen, J. D., and H. M. Brown. 1979. Comparison between free calcium selective microelectrodes and Arsenazo III. *In* Detection and Measurement of Free Ca^{2+} in Cells. C. C. Ashley and A. K. Campbell, editors. Elsevier/North-Holland Biomedical Press, New York. 395–408.

Ringbom, A. 1963. Complexation in Analytical Chemistry. John Wiley & Sons, Inc., Interscience Publishers, New York.

Rydqvist, B., and H. Mack Brown. 1980. Arsenazo III and phenol red as indicators of pH_i in *Balanus* photoreceptor. *Fed. Proc.* 39:2137.

Savvin, S. B. 1964. Analytical applications of Arsenazo III. III. The mechanism of complex formation between Arsenazo III and certain elements. *Talanta* 11:7–19.

Scarpa, A. 1979. Measurement of calcium ion concentrations with metallochromic indicators. *In* Detection and Measurement of Free Ca^{2+} in Cells. C. C. Ashley and A. K. Campbell, editors. Elsevier/North-Holland Biomedical Press, New York. 85–115.

Thomas, M. V. 1979. Arsenazo III forms 2:1 complexes with Ca and 1:1 complexes with Mg under physiological conditions. *Biophys. J.* 25:541–548.